TECHNICAL UNIVERSITY OF MUNICH

Limits on Kerr Nonlinearity and Photon Loss for the Initialization and Readout of a Kerr-cat Qubit

Bachelor's Thesis

by

Fabian Schatz

Academic Supervisor:
Stefan Filipp
Professorship for Technical Physics
Technical University of Munich

External Advisor:
Wolfgang Pfaff
Quantum Information Science Assistant Professor
University of Illinois at Urbana-Champaign

July 5, 2024

Acknowledgments

I would like to express my gratitude to Prof. Wolfgang Pfaff at the University of Illinois at Urbana-Champaign for the opportunity to work in his research group. Working with the team, including Philip Kim, Sam Cross, and other group members, has been an enriching experience. Their collaboration and support have been invaluable.

I also appreciate the learning opportunities provided, especially in the areas of superconducting qubits and quantum open systems. The knowledge and skills I gained during this time have significantly contributed to the development of my thesis and will undoubtedly aid me in my future career in physics.

Finally, I am grateful to Prof. Stefan Filipp at the Technical University of Munich (TUM) for his supervision and guidance during my thesis.

Abstract

This thesis explores the feasibility and limitations of initializing and reading out Kerr-cat qubits in systems with varying levels of Kerr nonlinearity (K) and photon loss rate (κ). Kerr-cat qubits, which use superpositions of coherent states (Schrödinger cat states), show promise for quantum computing due to their resilience to dephasing errors. This work investigates the quality of the initialization by simulating this process and analyzing the resulting Wigner function to identify unique quantum behavior. The primary challenge addressed is the need for high K and low Q, which is not achievable in all systems.

Contents

1 Introduction

Quantum computers perform computation on qubits, the quantum analogs to classical bits. Qubits can exist in a superposition of the computational basis states 0 and 1, such that we have a two-dimensional space of states (Bloch sphere). Quantum computers hold the potential for significant computational speedups for specific types of problems compared to classical computers.

Quantum systems can never be perfectly isolated; there is always some interaction with an environment with uncontrolled degrees of freedom. Therefore, over time, information about the qubit state is lost to that environment. The time during which a qubit can maintain its quantum state is called lifetime or coherence time. Decoherence is caused by relaxation and dephasing. Relaxation causes the excited state to decay to the ground state and dephasing disrupts the phase relation between those two states.

There are multiple ways to realize qubit systems. As an example, electrons can be used as a quantum qubit system with the spin-up and spin-down states as basis states. For quantum computing hardware, one popular approach is superconducting qubits, which utilize macroscopic-sized circuits. With this method, the quantum mechanical states can be represented by discrete Cooper-pair charge states in a specific type of superconducting circuit. A primary goal for making qubits is to have long coherence times. Eventually, we would like to perform many operations on a qubit before encountering an error. At a certain level of error suppression, we can use quantum error-correcting codes to make a quantum computer fault-tolerant.

It has been shown that there are more effective quantum error-correcting codes for "biased noise" (certain types of errors are suppressed, others increased). This gives rise to a particular type of superconducting qubit, the Kerr-cat qubit, which uses Schrödinger cat states, superpositions of coherent states. For the Kerr-cat qubit, dephasing is strongly suppressed. This is because the $|\pm X\rangle$ states of the Kerr-cat qubit are coherent states, which are eigenstates of the photon loss operator. However, their superpositions decay from photon loss, which leads to an increase in the bit-flip time. Still, it has been shown in [Gri+20] that the bit-flip rate increases linearly, whereas the phase-flip rate is suppressed exponentially in the photon number of the cat state.

Kerr-cat qubits have been made with high Kerr nonlinearity K and low photon loss rate κ. However, we might not have either available for some systems, so in this work, we will investigate the possibility of making Kerr-cat qubits for a broad range of values of K and quality factors Q (Q is related to κ with $Q = \frac{\omega}{\kappa}$ with ω the resonator frequency). Thus, this research explores the scope of quantum systems used to make a qubit, especially for systems that only offer low K, but better qubit control or coherence. Critically, we need to investigate if those systems still show unique qubit behavior, which can be measured as negativity in the Wigner function.

For quantum computing to have a useful qubit, we need to have knowledge of its state after computation. To gain information about a qubit state, we perform a quantum measurement, where the qubit state is projected onto a specific

basis. Superconducting qubits can be read out by observing and integrating the output field. For the Kerr-cat qubit, a readout procedure (Cat-quadrature readout) has been proposed [Gri+20] in which the qubit state is projected onto the basis of the coherent states (along the X-axis). This is a Quantum Non-Demolition readout (QND), meaning that the state is not destroyed during the measurement. Clearly, the state has to be read out before there is significant decoherence. Because we read out along the x-axis, this restricting time is the dephasing time. Again, the characteristic system parameters K and Q will influence the possibility of carrying out this readout, which we will investigate in this work.

In section 2, we go over the Kerr-cat Hamiltonian and discuss its energy eigenstates. Furthermore, we look at the Kerr-cat Hamiltonian in classical coordinates for some intuition. In section 3, we will explain how to simulate the initialization process of mapping the vacuum state in the nonlinear resonator to the even cat state by turning on the squeezing drive. Based on that, we examine how our system's characterizing parameters influence the initialization quality. Also, we discuss the approximations made and the validity of the results. In section 4, we will simulate the dephasing of the Kerr-cat qubit and calculate the Signal-to-noise ratio for the Cat-quadrature readout procedure. To conclude, in section 5, we discuss and comment on the implications of the obtained findings. In section A of the appendix, the underlying theory of coherent states, the basis states of the KCQ, is discussed. After that, in section B of the appendix, the theory of the methods used in the analysis of the Kerr-cat qubit is explained. Firstly (section B.1), there is the Wigner function, a quasi-probability distribution function used in quantum mechanics to represent the quantum state in phase space, combining position and momentum information. Secondly (section B.2, B.3 and B.4), the theory of open quantum systems is explained. In the last section of the appendix (section C), the *Python* code for the relevant results is presented.

2 Kerr-cat qubit

The Kerr-nonlinear resonator (KNR) Hamiltonian can be implemented using coherent microwave drives and 3- or 4-wave mixing (derivation for 3-wave mixing shown in [Gri+20]). It is given by:

$$\hat{H}_{\text{cat}}/\hbar = -K\hat{a}^{\dagger 2}\hat{a}^2 + \epsilon_2\left(\hat{a}^{\dagger 2} + \hat{a}^2\right) \tag{1}$$

$$= -K\left(\hat{a}^{\dagger 2} - \frac{\epsilon_2}{K}\right)\left(\hat{a}^2 - \frac{\epsilon_2}{K}\right) + \frac{{\epsilon_2}^2}{K} \tag{2}$$

In the expression of the Hamiltonian in equation (2), we can clearly see that the coherent states $|\alpha\rangle$ and $|-\alpha\rangle$ are degenerate energy eigenstates of the KNR Hamiltonian to eigenvalue $\frac{{\epsilon_2}^2}{K}$. That is also reasonable when considering the potential of the KNR in classical phase-space coordinates. As we see in figure 1 in the bottom plot, that potential has two stable extrema at $\alpha = \pm\sqrt{\frac{\epsilon_2}{K}}$.

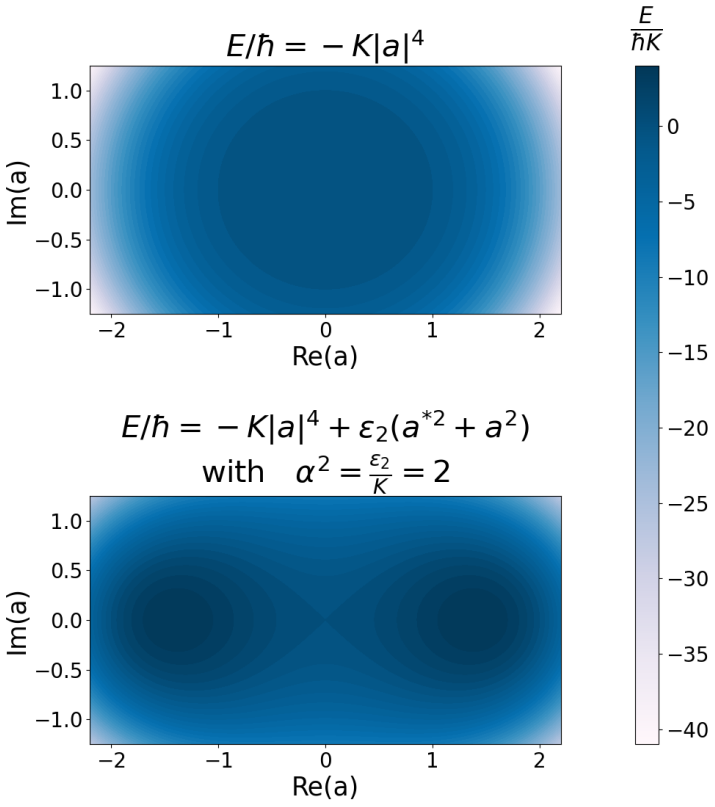

Figure 1: KNR in classical coordinates

In Supplementary Information section III of [Gri+20], they further show that in the by $\pm\alpha$ displaced frame, the Hamiltonian can be expressed as:

$$\hat{H}'/\hbar = -4K\alpha^2\hat{a}'^{\dagger}\hat{a}' \mp 2\alpha K(\hat{a}'^{\dagger 2}\hat{a}' + \hat{a}'^{\dagger}\hat{a}'^{2}) - K\hat{a}'^{\dagger 2}\hat{a}'^{2} \tag{3}$$

In the large α limit, the first term in the sum dominates, and we effectively have a harmonic oscillator potential. In this limit, the energy gap between the $|0\rangle$ and $|1\rangle$ states in the displaced frame is $E_{gap} = 4K\alpha^2$. Those states correspond to the states $D(\pm\alpha)\,|0\rangle$ and $D(\pm\alpha)\,|1\rangle$ in the original frame. However, for our application, we will not work within this limit. We can still have the approximation of the excited states $|\psi_e^{\pm}\rangle \approx (D(\alpha) \pm D(-\alpha))\,|1\rangle$ (corresponding to even and odd parity). Those excited states in our case have different energy levels, but we can use $4K\alpha$ as an estimate for the energy gap. For the exact energy gap, we would numerically diagonalize the Hamiltonian.

3 State initialization

By slowly ramping up the squeezing drive ϵ_2, we can map the "Fock qubit" onto the Kerr-cat qubit as shown in figure 2.

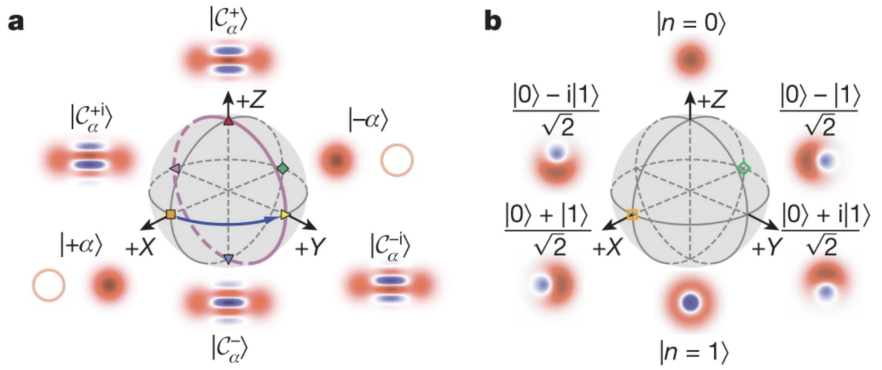

Figure 2: From [Gri+20]: **a**, Bloch sphere of the encoded Kerr-cat qubit, Wigner functions are shown for coherent states $|\pm X\rangle = |\alpha\rangle$ and their (here non-normalized) superpositions $|C_\alpha^\pm\rangle = (|\alpha\rangle \pm |-\alpha\rangle)/\sqrt{2}$ and $|C_\alpha^{\pm i}\rangle = (|\alpha\rangle \pm i\,|-\alpha\rangle)/\sqrt{2}$. **b**, Bloch sphere of the Fock qubit with Wigner function shown for the same states for comparison.

From the Adiabatic theorem ([SN20]: section 5.6 Hamiltonians with Extreme Time Dependence, paragraph Adiabatic Approximation) we know that the lowest degenerate eigenstates of the Fock qubit $|0\rangle$ and $|1\rangle$ are mapped to the lowest degenerate eigenstates of the Kerr-cat qubit. To suppress leakage into higher excited states, we need the ramp-up time to be much longer than $\frac{1}{2K}$.

Furthermore, during the whole time of the initialization of the Kerr-cat qubit, i.e., the squeezing drive ramp-up duration, the Hamiltonian commutes with the parity operator $\hat{P}$ because $\hat{a}^{\dagger 2}$ and $\hat{a}^2$ do (calculation shown for $\hat{a}^2$):

$$\hat{P}\hat{a}^2\hat{P}^{-1} = \hat{P}(\hat{a}\hat{a})\hat{P}^{-1} = (\hat{P}\hat{a}\hat{P}^{-1})(\hat{P}\hat{a}\hat{P}^{-1}) = (-\hat{a})(-\hat{a}) = \hat{a}^2 \tag{4}$$

Because H commutes with P at all times, also the time evolution operator $U(t) = \exp(\frac{-i}{\hbar}\int_0^t H(t')\,dt')$ does and we get for the state $|\psi(t)\rangle$ at time t of the initialization process:

$$P\,|\psi(t)\rangle = PU(t)\,|\psi(0)\rangle = U(t)P\,|\psi(0)\rangle = U(t)p\,|\psi(0)\rangle = p\,|\psi(t)\rangle \tag{5}$$

if $|\psi(0)\rangle$ is a parity eigenstate with eigenvalue p. Therefore, parity eigenstates remain eigenstates with the same eigenvalue during the initialization. That proves that the positive parity eigenstate $|0\rangle$ is mapped to the even Cat state and the negative parity eigenstate $|1\rangle$ to the odd Cat state and their superpositions accordingly.

For our research, we want to show that we can create a quantum state as a state of the Kerr-cat qubit without having a Fock qubit in the first place, but just the vacuum state $|0\rangle$.

Realization of the mapping We will ramp up the squeezing drive such that ϵ_2 follows a tanh evolution over time. Also, we would like to initialize the qubit as fast as possible without breaking the non-adiabatic limit. That is because there is a shorter period of photon loss, which causes bit-flips on the Y- and Z-axis of the Kerr-cat qubit. Because the adiabatic limit (ramp-up time much longer than $\frac{1}{2K}$) is dependent on K, it is reasonable to choose a timescale dependent on K for the evolution of the Hamiltonian. That is why we want to implement the Hamiltonian in equation (1) with a time-dependent $\epsilon_2(t)$:

$$\epsilon_2(t) = e_{2,final} \cdot \left[\frac{1}{2} \tanh\left(\left(t - \frac{4p_t}{K} \right) \cdot \frac{K}{p_t} \right) + \frac{1}{2} \right] \tag{6}$$

where p_t is a dimensionless parameter that characterizes the duration of the ramp-up.

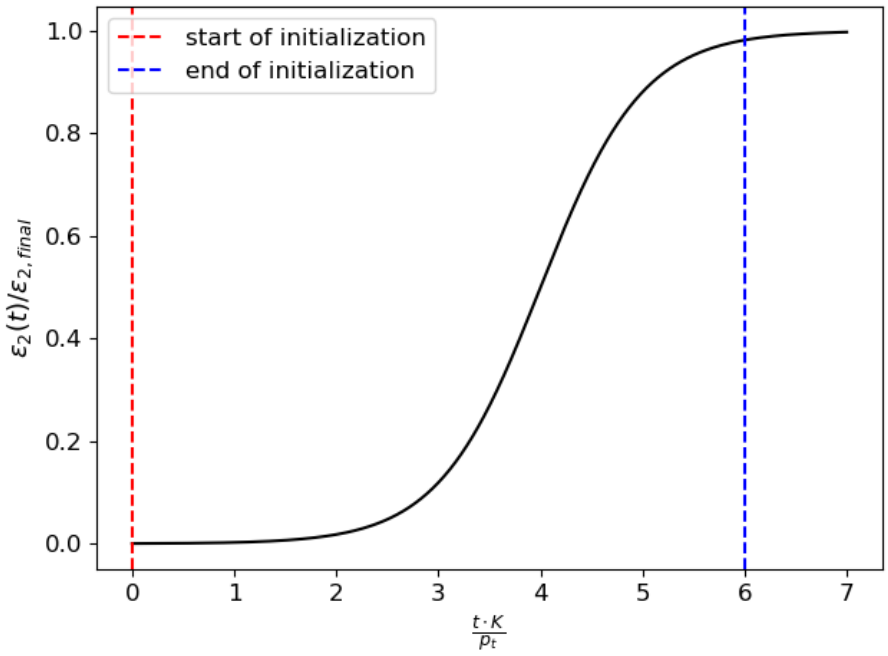

Figure 3: Adiabatic ramp-up of the squeezing drive over time of initialization $\tau \gg \frac{1}{2K}$

This ramp-up is illustrated in figure 3, and we will consider the $\tau \approx 6 \cdot p_t/K$. In this time interval, the squeezing drive is increased from around 0.03% to 98%

of the final value. We can start the initialization process at a slightly earlier or later time in the tanh ramp-up (without changing the initialization process) because at the beginning of the initialization, the state is approximately the vacuum state, which is not subject to photon loss.

For this thesis, $p_t = 2$, but in my code one can easily adjust that parameter. That way, we have a fast ramp-up while still ensuring adiabaticity as $\tau \approx \frac{12}{K} \gg \frac{1}{2K}$.

Wigner negativity of initialized state Eventually, we would like to use the initialized state as a Kerr-cat qubit, which means that we must be able to see the fringes in the Wigner function. Otherwise, the initialized state is just a statistical mixture of the two coherent states and essentially does not have quantum behavior (see section B.1.2). For a statistical mixture, we can not distinguish the $\pm Y$ and $\pm Z$ states of the KCQ. To measure Wigner negativity despite the error we make in the measurement, we would like to see for which characterizing values of Kerr nonlinearity K and quality factor Q (related to κ_a by $\kappa_a = \frac{\omega}{Q}$) we can get a particular maximal value for the Wigner negativity in the simulation. The higher this Wigner negativity is, the more likely we are to detect this negativity in the experiment. That would show that we initialized a state with unique quantum behavior and would be the first step of eventually using it as a Kerr-cat qubit.

For the initialization with specific values of K and Q, we maximize over the $\epsilon_{2,final}$ because we can adjust it by pumping the system in the experiment.

Modeling of the initialization process We model this process with the Lindblad master equation, where the dominant quantum jump operator is photon loss:

$$\dot{\rho}(t) = -\frac{i}{\hbar}[H_{cat,init}(t), \rho(t)] + \kappa_a(1 + n_{th})\mathcal{D}[\hat{a}]\rho(t) + \kappa_a n_{th}\mathcal{D}[\hat{a}^\dagger]\rho(t) \quad (7)$$

where $\mathcal{D}[\hat{O}]\hat{\rho} = \hat{O}\hat{\rho}\hat{O}^\dagger - \frac{1}{2}(\hat{O}^\dagger\hat{O}\hat{\rho} + \hat{\rho}\hat{O}\hat{O}^\dagger)$ and n_{th} is the equilibrium occupation number of the $|1\rangle$ state in contact with a thermal bath and is negligible in our case.

Dependence of Wigner negativity on product $K \cdot Q$ Let us assume we found a solution to equation (7) for parameters K and Q with ϵ_2 set, such that $\rho(t)$ at the end of the initialization has maximum Wigner negativity. We will show in the following that if there is $\tilde{K}$ and $\tilde{Q}$ such that $K \cdot Q = \tilde{K} \cdot \tilde{Q}$, optimizing final Wigner negativity leads us to the same result as before. Final Wigner negativity is therefore only dependent on the product $K \cdot Q$.

Proof. Let ρ_0 be the solution for equation (7):

$$\frac{d\rho_0(t)}{dt} = F(\rho_0(t), t) \quad (8)$$

where $F(\rho_0(t), t)$ represents the right side of equation (7) and the time dependence is caused by the time-dependent Hamiltonian.
Because of the invariant product, we write:

$$\tilde{K} = \gamma K \quad \text{and} \quad \tilde{\kappa_a} = \frac{\omega}{\tilde{Q}} = \gamma \kappa_a \tag{9}$$

We can now pick $\tilde{\epsilon_2} = \gamma \epsilon_2$ and the new differential equation becomes:

$$\frac{d\tilde{\rho} f(t)}{dt} = \gamma F(\tilde{\rho}(t), \gamma t) \tag{10}$$

because the argument in the time-dependent Hamiltonian is linearly proportional to K.

Then $\tilde{\rho}(t) = \rho_0(\gamma t)$ is a solution to this equation because it has the same initial state and:

$$\frac{d\rho_0(\gamma t)}{dt} = \frac{d\rho_0(\gamma t)}{d(\gamma t)} \cdot \gamma = \gamma F(\rho_0(\gamma t), \gamma t) \tag{11}$$

Now, as the new time for initialization $\tilde{\tau} = \frac{\tau}{\gamma}$, the end state of initialization and, hence, the Wigner negativity is the same as before. It is easy to show that another $\tilde{\epsilon_2}$ will not initialize a state with greater negativity.

Physically, the initialization evolution is accelerated by a factor of γ. But, the initialization time is shrunk to a factor of $\frac{1}{\gamma}$, which initializes the same state. □

3.1 *Qutip* simulation

For the simulations in *qutip* we solve the Lindblad master equation numerically with *qutip.mesolve* with the jump operator $\sqrt{\kappa_a}\hat{a}$. For simplicity, we always initialize a $|\alpha\rangle$ with real α and then take the values of the Wigner function $W(z)$ for $Re(z) = 0$. Intuitively, this gives a profile of the fringes in the Wigner function, from which we take the minimum value. For given K and Q, we optimize this value over all $\epsilon_{2,final}$ to get the optimal value for given Kerr nonlinearity K and quality factor Q.

We truncate the expansion of the cat state in Fock states for the numerical simulations at the 30th Fock state. Still, those simulations are computationally intensive because we are solving differential equations for each density matrix element. However, assuming a perfectly adiabatic process can simplify this problem.

3.2 Calculation for adiabatic evolution

Again, we use the *qutip* convention of the Wigner function.

There are two processes that, as we will see, independently influence Wigner negativity: photon loss and increase of α due to the squeezing drive ramp-up.

Increase of α due to the squeezing drive ramp-up From equation (58) in *qutip* convention, we get maximum negativity for $Re(z) = 0$ and $\frac{4}{\sqrt{2}} Im(z)\alpha = \pi$. We can express the maximum Wigner negativity $n(\alpha)$ of the even $|\alpha\rangle$ cat state (neglecting the exponentially in α^2 suppressed Gaussian parts of the Wigner function) as:

$$n(\alpha) = \frac{1}{\pi(1 + e^{-2\alpha^2})} e^{-2(\frac{\pi}{4\alpha})^2} \tag{12}$$

From now, we will refer to maximum negativity in the Wigner function as simply Wigner negativity. To find a differential equation governing the time evolution, we evaluate how Wigner negativity changes in an infinitesimal increment $d\alpha$. We neglect the exponentially suppressed part of the normalization $e^{-2\alpha^2}$.

$$\begin{aligned} n(\alpha + d\alpha) &= n(\alpha) \cdot \frac{e^{-2(\frac{\pi}{4(\alpha+d\alpha)})^2}}{e^{-2(\frac{\pi}{4\alpha})^2}} = n(\alpha) \cdot \frac{e^{-2(\frac{\pi}{4\alpha})^2 \cdot (1 - 2\frac{d\alpha}{\alpha} + O(d\alpha^2))}}{e^{-2(\frac{\pi}{4\alpha})^2}} \\ &= n(\alpha) \cdot \exp(\frac{\pi^2}{4\alpha^3} d\alpha + O(d\alpha^2)) = n(\alpha) \cdot (1 + \frac{\pi^2}{4\alpha^3} d\alpha + O(d\alpha^2)) \end{aligned} \tag{13}$$

This is equivalent to:

$$\frac{dn}{d\alpha} = \frac{\pi^2}{4\alpha^3} n \tag{14}$$

Using

$$\alpha^2 = \frac{\epsilon_2}{K} = \frac{\epsilon_{2,final}}{K} \cdot \left[\frac{1}{2} \tanh\left(\left(t - \frac{4p_t}{K} \right) \cdot \frac{K}{p_t} \right) + \frac{1}{2} \right] \tag{15}$$

we get a differential equation in t:

$$\frac{dn}{dt} = n \cdot \frac{\pi^2 \epsilon_{2,final}}{16 p_t \alpha^4} \left[1 - \tanh^2\left((t - \frac{4p_t}{K}) \cdot \frac{K}{p_t} \right) \right] \tag{16}$$

Photon loss In this section, we will examine how the state's Wigner negativity evolves in a time step dt due to photon loss. We can write the state's density matrix at all times as

$$\rho_a = \frac{1}{2(1 + e^{-2|\alpha^2|})} \Big(|\alpha\rangle\langle\alpha| + b|-\alpha\rangle\langle\alpha| + b|\alpha\rangle\langle-\alpha| + |-\alpha\rangle\langle-\alpha| \Big) \tag{17}$$

This is true because the vacuum state in the beginning can be written in this way with $\alpha = 0$ and $b = 0$, the squeezing drive ramp-up increases the value of α, and the process of photon loss only decreases the value of b as we will see in this paragraph (we can look at these processes independently). With the Lindblad master equation, we have:

$$\begin{aligned} \frac{d\rho_a}{dt} &= -\frac{i}{\hbar}[H, \rho_a] + \kappa_a \hat{a} \rho_a \hat{a}^\dagger - \frac{1}{2} \hat{a}^\dagger \hat{a} \rho_a - \frac{1}{2} \rho_a \hat{a}^\dagger \hat{a} \\ &= \kappa_a \alpha^2 \Big(|\alpha\rangle\langle\alpha| - b|-\alpha\rangle\langle\alpha| - b|\alpha\rangle\langle-\alpha| + |-\alpha\rangle\langle-\alpha| - \rho_a \Big) \\ &= -2\kappa_a \alpha^2 b \Big(|\alpha\rangle\langle-\alpha| + |-\alpha\rangle\langle\alpha| \Big) \end{aligned} \tag{18}$$

From here, we can realize that only the parameter b changes for the process of photon loss. Then with:

$$\frac{d\rho_a}{dt} = \dot{b}\Big(|\alpha\rangle \langle -\alpha| + |-\alpha\rangle \langle \alpha| \Big) \tag{19}$$

we have:

$$\dot{b} = -2\kappa_a \alpha^2 b \tag{20}$$

The fringes in the Wigner function are caused solely by the off-diagonal elements in the basis of the coherent states and are directly proportional to b. Hence, we get a differential equation for Wigner negativity due to photon loss:

$$\begin{aligned} \frac{dn}{dt} &= -2\kappa_a \alpha^2 n \\ &= -n\frac{\epsilon_2}{K}\Big[\tanh\Big((t - \frac{4p_t}{K}) \cdot \frac{K}{p_t}\Big) + 1\Big] \cdot \kappa_a \end{aligned} \tag{21}$$

Complete differential equation We can clearly see that the change of α due to the slowly evolving Hamiltonian and photon loss are independent processes in the increment dt. We can add their effects in that time interval.

The time evolution of Wigner negativity for adiabatic evolution state is determined by:

$$\frac{dn}{dt} = n \cdot \frac{\pi^2 \epsilon_{2,final}}{16 p_t \alpha^4}\Big[1 - \tanh^2\Big(t - \frac{4p_t}{K}) \cdot \frac{K}{p_t}\Big)\Big] - n\frac{\epsilon_2}{K}\Big[\tanh\Big((t - \frac{4p_t}{K}) \cdot \frac{K}{p_t}\Big) + 1\Big] \cdot \kappa_a \tag{22}$$

Starting point of numerical integration At the beginning of the initialization simulation, the state's photon number is small, and therefore, photon loss is exponentially suppressed. At time $3 * p_t/K$, the squeezing drive is only ramped up to $0.12 \cdot \epsilon_{2,final}$. In our range of photon numbers ($\bar{n} < 10$), photon loss is still negligible before this time. This way, we can start the numerical integration at that point in time and calculate the negativity until that time only through the increase in α. We calculate Wigner negativity $neg(t)$ at that time:

$$neg(\frac{3p_t}{K}) = \frac{1}{\pi} e^{-2(\frac{\pi}{4\alpha(\frac{3p_t}{K})})^2} = \frac{1}{\pi} e^{-\frac{\pi^2 K}{4\epsilon_{2,final}(\tanh(-1)+1)}} \approx \frac{1}{\pi} e^{-\frac{\pi^2 K}{4 \cdot 0.24 \epsilon_{2,final}}} \tag{23}$$

We cannot set the starting value at an earlier point in time because the Wigner negativity values are minimal, which leads to a numerical error when performing the integration.

Additional note Because the processes of photon loss and increasing Wigner negativity of the $|\alpha\rangle$ state are independent, we do not have to include the latter effect into the differential equation, but calculate it with equation (12). This would be a more elegant way of calculating the negativity but does not significantly change the results. The modification to the code that generates figure 4 is shown in appendix C.3.

3.3 Results

In figure 4, the optimized Wigner negativity of the end state is presented for both methods of simulating the initialization process. Wigner negativity is plotted against the characterizing parameter $K \cdot Q$. Both methods give very similar results; at most, there is a difference of about 15% between them.

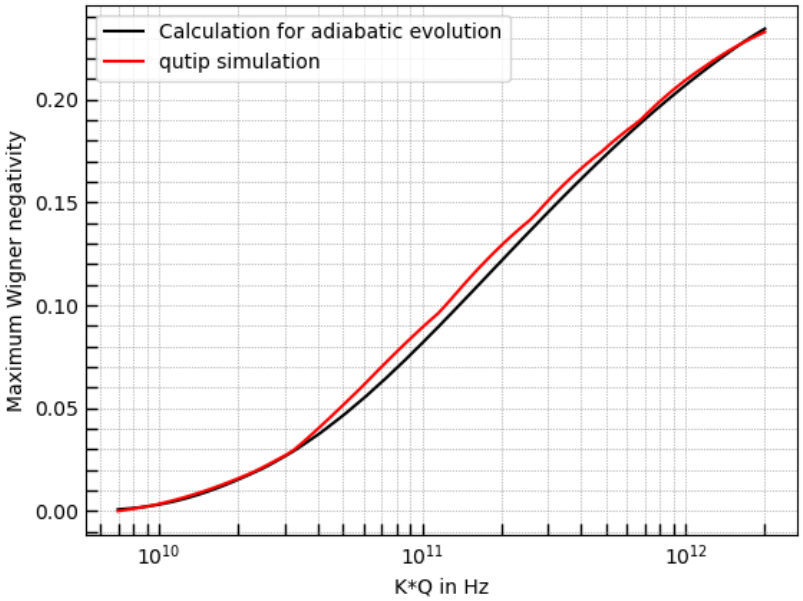

Figure 4: Maximum negativity in the Wigner function of the initialized state given a system with characterizing values K and Q (code shown in appendix C.1 and C.2)

In the following paragraph, we discuss the validity of the simulation and analyze the errors made. To begin with, for the state initialization, we note that for the *qutip* simulation there are errors because we only take the maximal negativity on the $Re(a) = 0$ axis of the Wigner function graph, the error of Fock state truncation and the numerical error. We get a last error for both ways of the simulation from the assumption that the system only experiences the dominant loss process, photon loss. All those errors are extremely small, and we can assume these *qutip* simulation results to be exact. For the calculation with the assumption of an adiabatic process, we simplify the Wigner function as discussed in 3.2. This approximation causes an error of $\approx 20\%$ for $\alpha = 1$ and is exponentially suppressed in α^2. This error could be corrected in a future investigation. Another error arises from the inaccurate starting point of the numerical integration, which is negligible. The last error originates from the

non-adiabaticity but is hard to quantify. However, we see that both graphs in figure 4 match up very well, suggesting that adiabaticity is a valid assumption within the error margin we attempt.

The final photon number for the initialization with the highest Wigner negativity is given in figure 5. Again, the results from both methods of simulating the process are shown. They match up very well in general. However, the simplification in the Wigner function we make for the calculation is not true for small values of the final photon number. That is why the results for small values of $K \cdot Q$ are wrong in the calculation and do not align with the results of the *qutip* simulation.

Furthermore, we can see small jumps in the graph for the *qutip* simulation. This is due to some numerical approximations and the non-adiabaticity. Also, all the errors in the Wigner negativity obviously influence the error in the photon number. Those imperfections do not matter much because for a photon number close to the optimal one, we expect to initialize a state with almost the same Wigner negativity.

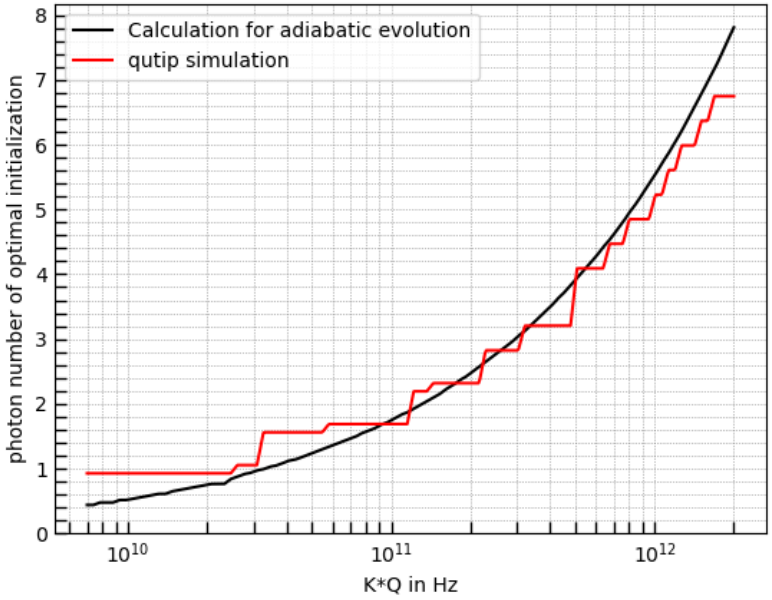

Figure 5: Photon number of the initialized state for which maximum negativity is achieved

To make a more comprehensive plot, figure 6 has height lines for certain values of end state Wigner negativity on an underlying grid of K and Q. That

way, we can see the effect of each parameter independently.

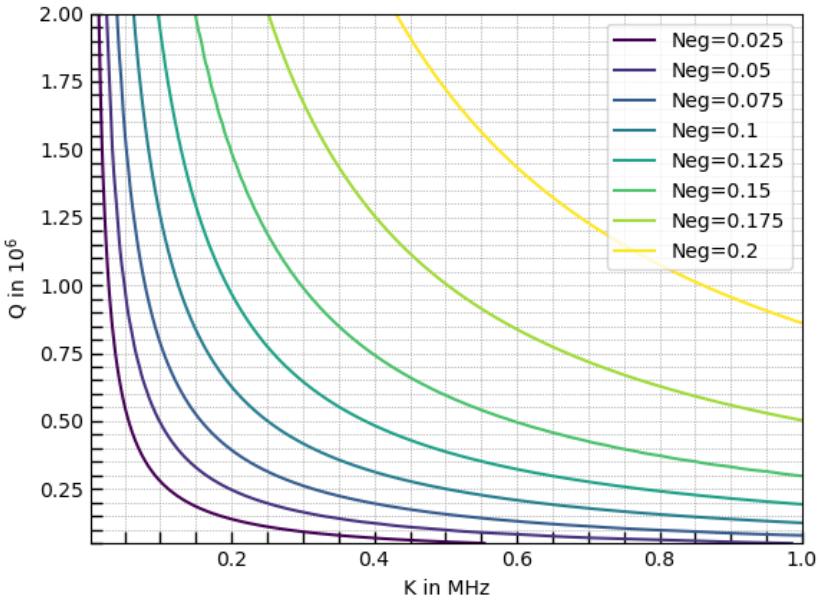

Figure 6: Maximum negativity in the Wigner function of the initialized state given a system with characterizing values K and Q; visualization as a three-dimensional plot with Wigner negativity as height values on a two-dimensional K-Q grid (only lines of equal Wigner negativity are shown)

4 Cat-quadrature (CQ) readout

To read out the state of the Kerr-cat qubit, we could first think of mapping the KCQ back to the Fock qubit by slowly turning off the squeezing drive. However, this readout destroys the state for subsequent operations on the qubit. Readout procedures, in which the qubit is not destroyed, are called quantum non-demolition (QND) readouts. One such method is the "cat-quadrature readout" (CR), proposed in [Gri+20]. The idea is to generate a swap interaction between the Kerr nonlinear resonator and a readout cavity, which, for long times, swaps the states of the two systems back and forth. With this, we cause the KCQ to get projected onto the $|\pm\alpha\rangle$ states and cause a coherent drive on the readout cavity. The state in the readout cavity will approximately transform to the state of the KNR, and we can measure the state by observing the emitted cavity field. If we choose the leakage from the cavity to be much greater than the coupling strength, we can avoid unwanted back reaction on the KCQ.
By applying an additional drive to our system together with 3-wave or 4-wave mixing, we can implement this relevant swap term that adds to the Hamiltonian:

$$\hat{H}_{\mathrm{cr}}/\hbar = ig_{cr}(\hat{a}\hat{b}^\dagger - \hat{a}^\dagger\hat{b}) \tag{24}$$

When the KCQ is in the coherent $|\pm\alpha\rangle$ state, this interaction effectively induces a coherent drive on the cavity. Then:

$$\hat{H}_{\mathrm{cr}}/\hbar \approx \pm ig_{cr}\alpha(\hat{b}^\dagger - \hat{b}) \tag{25}$$

4.1 Measurement

In order to assign a value to the measurement outcome, we integrate the signal b_{out} over the measurement time τ. For the current analysis, we do not use a filter to improve the readout signal, and the measurement operator reads:

$$\hat{M}(\tau) = \sqrt{\kappa_b}\int_0^\tau dt\,\left(b_{\mathrm{out}} + b_{\mathrm{out}}^\dagger\right) \tag{26}$$

where κ_b is the photon loss rate of the readout cavity.

4.1.1 Signal-to-Noise ratio (SNR) calculation

We can solve the dynamics of the readout cavity with the quantum Langevin equation.

$$\partial_t\hat{b} = \frac{i}{\hbar}[\hat{H}_{cr},\hat{b}] - \frac{\kappa_b}{2}\hat{b} - \sqrt{\kappa_b}\,\hat{b}_{in} \approx \pm g_{cr}\alpha - \frac{\kappa}{2}\hat{b} - \sqrt{\kappa_b}\,\hat{b}_{in} \tag{27}$$

Taking expectation values on both sides, we conclude with the readout cavity initially being in the vacuum state:

$$\partial_t\langle\hat{b}\rangle =: \partial_t\beta = \pm g_{cr}\alpha - \frac{\kappa_b}{2}\beta \implies \beta_\pm(t) = \pm\frac{2g_{cr}\alpha}{\kappa_b}[1 - e^{-\frac{\kappa_b t}{2}}] \tag{28}$$

With this, we can now compute the average signal of this measurement. Note that from the input-output relation, we get $\langle b_{out}\rangle = \langle b\rangle$.

$$\begin{aligned}\langle M\rangle_{+X} - \langle M\rangle_{-X} &= \left[\sqrt{\kappa_b}\int_0^\tau dt\ \langle b_{\rm out}\rangle + \langle b_{\rm out}^\dagger\rangle\right]_{-X}^{+X} \\ &= \kappa_b \int_0^\tau dt\ \left(\beta_+(t) + \beta_+(t)^\dagger - \beta_-(t) + \beta_-(t)^\dagger\right) \\ &= 8g_{cr}\alpha\int_0^\tau dt\ (1 - e^{-\frac{\kappa_b t}{2}}) \\ &= 8g_{cr}\alpha\tau\ [1 - \frac{2}{\kappa_b\tau}(1 - e^{-\frac{\kappa_b\tau}{2}})] \end{aligned} \tag{29}$$

The fundamental quantum noise is $\langle \hat{M}_N^2(\tau)\rangle = \langle(\hat{M} - \langle\hat{M}\rangle)^2\rangle = \kappa_b\tau$.

We finally get a signal-to-noise ratio (SNR) in terms of integration time τ of:

$$\text{SNR} \equiv \sqrt{\frac{|\langle\hat{M}\rangle_{+X} - \langle\hat{M}\rangle_{-X}|^2}{\langle\hat{M}^N_{+X}(\tau)\rangle + \langle\hat{M}^N_{-X}(\tau)\rangle}} = 4\sqrt{2}g_{cr}\alpha\frac{\sqrt{\kappa_b\tau}}{\kappa_b}\ [1 - \frac{2}{\kappa_b\tau}(1 - e^{-\frac{\kappa_b\tau}{2}})] \tag{30}$$

For visualization, the SNR values are shown versus readout integration time for sample values in figure 7.

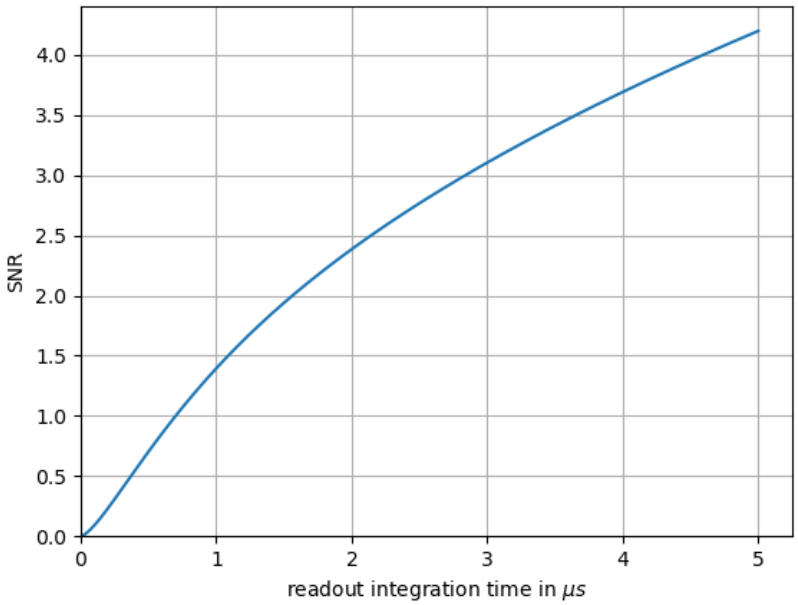

Figure 7: SNR plotted for sample values of $\alpha = \sqrt{2}$, $g_{cr} = 1 \cdot 10^5$ Hz and $\kappa_b = 1 \cdot 10^6$ Hz

4.2 Kerr-cat qubit dephasing time

The integration time available for the readout is restricted by the KCQ dephasing time, during which the two different possible post-measurement states decay and thus can not be distinguished anymore.

We can phenomenological describe this decay again with the master equation:

$$\dot{\rho}(t) = -\frac{i}{\hbar}[H_{KCQ}(t), \rho(t)] + \kappa_a \mathcal{D}[\hat{a}]\rho(t) + \kappa_a n_{th} \mathcal{D}[\hat{a}^\dagger]\rho(t) + \kappa_{eff} \mathcal{D}[\hat{a}^\dagger \hat{a}] \quad (31)$$

Those processes cause out-of-manifold leakage out of the KCQ Bloch sphere. For the measurement, the x-expectation is relevant as this value is integrated over time. The time evolution of the dephasing of the $|\alpha\rangle$ state is simulated using *qutip.mcsolve*, which is a numerical technique to solve the master equation. The x-expectation value at each time step is returned.

We do not have a perfect exponential decay, but it is a good estimate. Therefore, we fit an exponential decay of the x expectation value to get the dephasing time.

To get an idea of the order of magnitude of the dephasing times for certain K and Q and to test the simulation, we use the parameters $n_{th} = 0.08$ and

κ_{eff} = 230Hz from [Gri+20] to plot dephasing time values on a K-Q grid. These results are shown in figure 8.

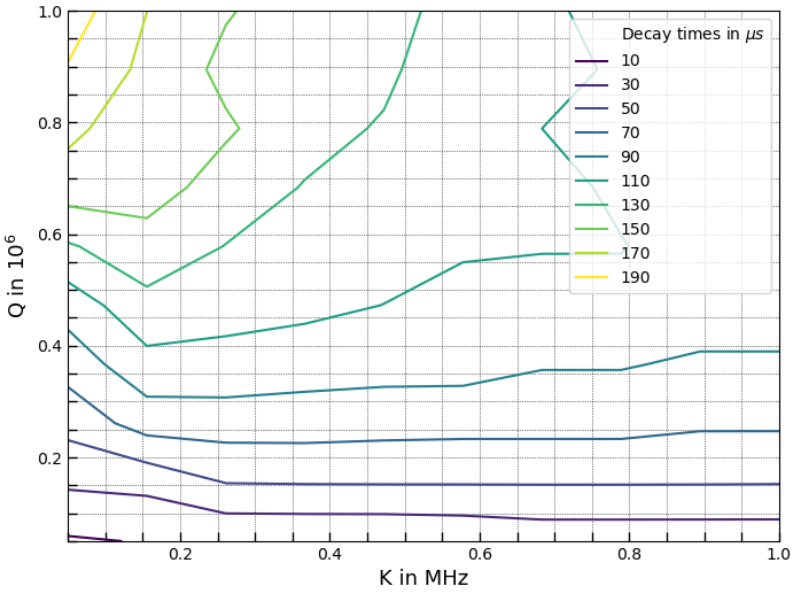

Figure 8: Dephasing time of the KCQ (decay time of the initialized $|\pm\alpha\rangle$ state) for initialized state with system parameters K and Q (initialized state with maximum Wigner negativity was chosen)

It is, however, more beneficial for further analysis to plot the dephasing decay constant (inverse of decay time) for one main reason. We have two noise processes that mainly cause the dephasing. Those are $a^\dagger a$ and $a^\dagger$ noise. Both approximately cause an exponential decay of the x-expectation value, and we can simulate them independently. Then, when both effects happen, the decay constants of the individual simulations add up. Also, the decay constants should be linearly proportional to the noise rate. Obviously, those statements are made with assumptions of perfect exponential decay of the x-expectation value and that the noise processes do not interfere with each other. In fact, in the simulations, we can observe this linear increase of the decay constants when increasing the noise rate. The addition of decay constant for the superposition of the two noise processes can also be seen. To what extent we can make this assumption needs further investigation.

In figures 9 and 10 the dephasing decay constants are plotted on a K-Q as before for the dephasing time.

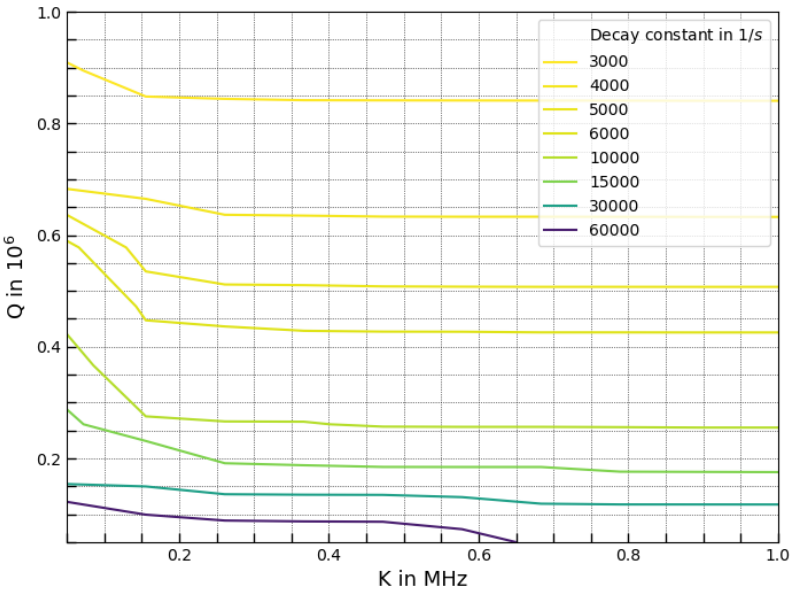

Figure 9: Decay constant for the dephasing of the KCQ for initialized state with system parameters K and Q (initialized state with maximum Wigner negativity was chosen), $n_{th} = 0.08$ and $\kappa_{eff} = 0$

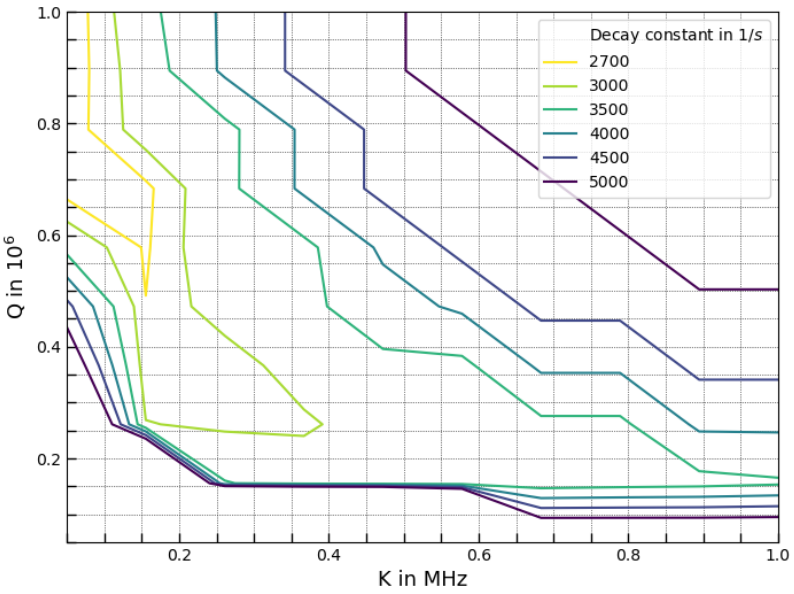

Figure 10: Decay constant for the dephasing of the KCQ for initialized state with system parameters K and Q (initialized state with maximum Wigner negativity was chosen), $n_{th} = 0$ and $\kappa_{eff} = 230$ Hz

In the following, we simulate both noise processes at the same time (same simulation as in figure 8), and we can already see that we get the resulting dephasing decay constants roughly from adding up the two graph for the individual noise processes. The color scales are the same for figure 9 and 11. For figure 10, the color scale is adjusted such that the discernibility of the lines is increased.

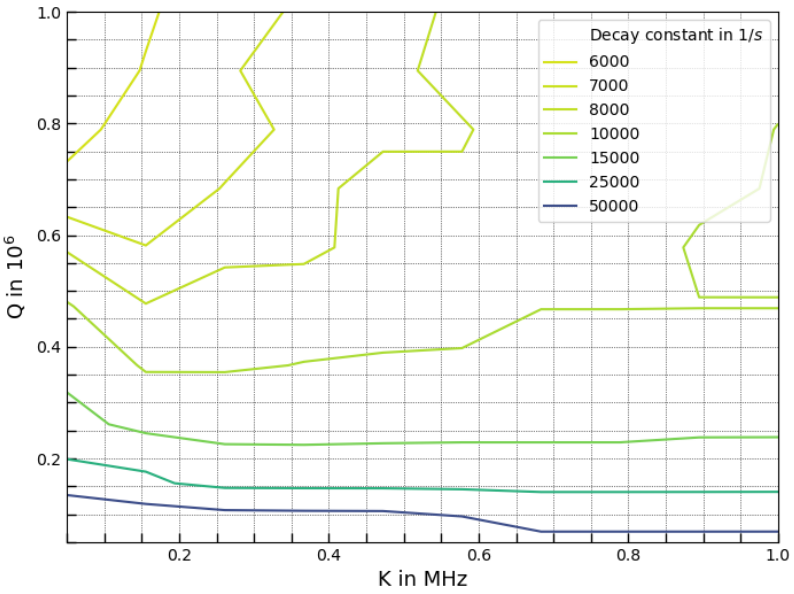

Figure 11: Decay constant for the dephasing of the KCQ for initialized state with system parameters K and Q (initialized state with maximum Wigner negativity was chosen), $n_{th} = 0.08$ and $\kappa_{eff} = 230$ Hz (code is shown in appendix C.4)

5 Conclusion

In this thesis, we explored the scope of quantum systems used to make a Kerr-cat qubit depending on their Kerr nonlinearity K and photon loss rate κ. We investigated if those systems still show unique qubit behavior, which can be measured as negativity in the Wigner function. Additional, we studied the realizability of the CQ readout in this parameter regime.

To start with, we found one very accurate way and another more computationally efficient way of simulating Wigner negativity of an initialized Kerr-cat qubit. Considering the feasibility of the initialization, as shown in section 3.3, we would most probably need a value of at least $K \cdot Q = 5 \cdot 10^{10} - 1 \cdot 10^{11}$ Hz to measure negativity in the Wigner function to prove that we can at least initialize a state with characteristic, unique quantum behavior.

Considering the CQ readout, we calculated a formula of SNR per integration (30) for a particular set of parameters. For reasonable parameters of g_{cr} and κ_b, we can achieve a signal-to-noise ratio in the order of a microsecond.

Additionally, we can simulate the dephasing process of the Kerr-cat qubit for different noise processes. Using the parameters from [Gri+20] as in figure 8, we can see that this readout can be carried out achieving a SNR of $1 - 2$ in a fraction of $\frac{1}{50}$ of the dephasing time if $Q > 200.000$. This shows that there is a large range in K and Q, such that the initialized Kerr-cat qubit would be useful in the sense that we can read out its state reliably. It is important to note that we will not achieve this exact SNR due to external noise effects (for example electronic noise).

One important takeaway is that we can strongly increase the dephasing time if we cool down the qubit more than as it was done in [Gri+20] because in our case the dephasing time is mainly limited by $\hat{a}^\dagger$ noise (for parameters as in [Gri+20]) which is related to the environment's temperature.

In conclusion, this thesis proposes values for K and Q, where further investigation of Kerr-cat qubits is sensible. Additionally, it provides a detailed analysis of the initialization and the CQ readout procedure both dependent on K and Q. The simulations can be utilized for visualization as well as for further research.

References

[Gri+20] A. Grimm et al. "Stabilization and operation of a Kerr-cat qubit". In: *Nature* 584.7820 (Aug. 2020), pp. 205–209. ISSN: 1476-4687. DOI: 10.1038/s41586-020-2587-z. URL: http://dx.doi.org/10.1038/s41586-020-2587-z.

[HR06] Serge Haroche and Jean-Michel Raimond. *Exploring the Quantum: Atoms, Cavities, and Photons*. Oxford University Press, Aug. 2006. ISBN: 9780198509141. DOI: 10.1093/acprof:oso/9780198509141.001.0001. URL: https://doi.org/10.1093/acprof:oso/9780198509141.001.0001.

[Hud74] R.L. Hudson. "When is the wigner quasi-probability density non-negative?" In: *Reports on Mathematical Physics* 6.2 (1974), pp. 249–252. ISSN: 0034-4877. DOI: https://doi.org/10.1016/0034-4877(74)90007-X. URL: https://www.sciencedirect.com/science/article/pii/003448777490007X.

[SN20] J. J. Sakurai and Jim Napolitano. *Modern Quantum Mechanics*. 3rd ed. Cambridge University Press, 2020.

[Ste07] D.A. Steck. *Quantum and Atom Optics*. 2007. URL: https://books.google.com/books?id=bc9TMwEACAAJ.

[ZG97] Peter Zoller and C. W. Gardiner. *Quantum Noise in Quantum Optics: the Stochastic Schrödinger Equation*. 1997. arXiv: quant-ph/9702030 [quant-ph].

Appendix

A Theory of coherent states

Because of the Correspondence principle, we expect the existence of quantum states that resemble the classical motion in the harmonic oscillator. The closest resemblance is given by coherent states, which are displaced vacuum states. Their Gaussian probability distribution in position and momentum has the minimum uncertainty due to Heisenberg's uncertainty principle.

For clarity, we will denote coherent states as $|\alpha\rangle_C$ and Fock states as $|n\rangle_F$ in this section.

For $\alpha = x + ip$ the coherent states $|\alpha\rangle_C$ is:

$$\begin{aligned} |\alpha\rangle_C &= \mathrm{D}(\alpha)\,|0\rangle_F = e^{\alpha\hat{a}^\dagger - \alpha^*\hat{a}}\,|0\rangle_F = e^{-\frac{|\alpha|^2}{2}} e^{\alpha\hat{a}^\dagger} e^{-\alpha^*\hat{a}}\,|0\rangle_F \\ &= e^{-\frac{|\alpha|^2}{2}} \sum_{n=0}^{\infty} \frac{\alpha^n}{n!}\hat{a}^\dagger\,|0\rangle_F = e^{-\frac{|\alpha|^2}{2}} \sum_{n=0}^{\infty} \frac{\alpha^n}{\sqrt{n!}}\,|n\rangle_F \end{aligned} \tag{32}$$

For further review, refer to section 3.1.3 of [HR06].

B Methods

This section discussing the methods used for the analyses in my thesis is oriented by [HR06] and [Ste07]. Those are highly recommended for further review.

B.1 Wigner distribution

The Wigner distribution is an essential tool for analyzing quantum states and capturing the non-classical behavior. A classical state can be represented as a point in phase space by its position and conjugate momentum. Statistical uncertainty and lack of knowledge are accounted for by substituting points in phase space with a probability distribution. Describing a state in phase space is helpful because the state's evolution is determined completely by Hamilton's equations of motion if the state's representation in phase space is given at a particular time. A quantum extension of this representation is the Wigner quasiprobability distribution. Because Heisenberg's uncertainty relation forbids the simultaneous measurement of both position x and momentum p, there is no quantum phase space probability distribution in the same sense as in classical physics. For classical states, the statistical average of an observable $o(x,p)$ is given by:

$$\bar{o} = \int f(x,p)o(x,p)\,dx\;dp \tag{33}$$

for the state´s probability distribution f. This is a property the Wigner distribution will also have.

The Wigner distribution is expressed in terms of the density matrix:

$$W(\alpha) = \frac{1}{\pi^2}\int d^2\lambda C_S(\lambda)\exp(\alpha\lambda^\star - \alpha^\star\lambda) \tag{34}$$

where $C_S(\lambda)$ is the symmetric order characteristic function.

$$C_S(\lambda) = \langle D(\lambda)\rangle = \mathrm{Tr}[\rho e^{\lambda\hat{a}^\dagger - \lambda^\star\hat{a}}] \tag{35}$$

For this theory section, we will stick to this widely used definition/convention because it is more intuitive, but at the end of subsection B.1.3, we will go over the convention that is used in this work and in the Python library *qutip* that is used for simulations in this work.

There is another equivalent form for the Wigner distribution, which is given by:

$$W(x,p) = \frac{1}{\pi}\int_{-\infty}^{\infty} dx'\; e^{-2ipx'}\,\langle x + \frac{x'}{2}|\,\rho\,|x - \frac{x'}{2}\rangle \tag{36}$$

B.1.1 Properties

Average operator value As stated before, the Wigner distribution should conserve the property of a classical phase space probability distribution that averages of operators can be computed by integration as in (33).

First, the quantum operator $O(a, a^\dagger)$ (expressed as a function of $\hat{a}$ and $\hat{a}^\dagger$) is written as an integral with the complex function that corresponds to the given operator:

$$O(\hat{a}, \hat{a}^\dagger) = \int d^2\alpha \; o(\alpha, \alpha^\star)\delta(\alpha - \hat{a}) \tag{37}$$

Note that one complex function $o(\alpha, \alpha^\star)$ can naively correspond to more than one operator. This expression is only true if $O(\hat{a}, \hat{a}^\dagger)$ is in symmetric order (operator expression is symmetric with respect to operators $\hat{a}$ and $\hat{a}^\dagger$). With the definition of the Wigner distribution ((34) and (35)) it can be compactly written as:

$$W(\alpha) = \frac{1}{\pi^2}\mathrm{Tr}\Big[\rho \int d^2\lambda \, e^{\lambda^*(\alpha-\hat{a})-\lambda(\alpha^*-\hat{a}^\dagger)}\Big] \tag{38}$$

With the Dirac δ-distribution as the Fourier transform of the constant function, we have:

$$W(\alpha) = \mathrm{Tr}\big[\rho\delta(\alpha - \hat{a})\big] \tag{39}$$

We can understand the Wigner function as an extension and combination of the probability distribution in position and momentum space as we get for the probability distribution in position space $P(x)$ and similarly for momentum space:

$$P(x) = \langle x|\,\hat{\rho}\,|x\rangle = \mathrm{Tr}[\hat{\rho}\,|x\rangle\,\langle x|] = \mathrm{Tr}[\hat{\rho}\int dx'\delta(x'-x)\,|x'\rangle\,\langle x'|] = \mathrm{Tr}[\hat{\rho}\delta(\hat{x}-x)] \tag{40}$$

Finally, we can get for the average operator value:

$$\langle O\rangle = \mathrm{Tr}[\rho O] = \int d^2\alpha\, o(\alpha,\alpha^*)\,\mathrm{Tr}[\rho\,\delta(\alpha-\hat{a})] = \int d^2\alpha\, o(\alpha,\alpha^*)\,W(\alpha) \tag{41}$$

Relation to position and momentum distribution As an extension for the probability distribution in one quadrature, those can be recovered from the Wigner distribution by:

$$P(x) = \langle x|\rho|x\rangle = \int dp\, W(x,p) \tag{42}$$

$$P(p) = \langle p|\rho|p\rangle = \int dx\, W(x,p) \tag{43}$$

Overlap of two Wigner distributions

$$
\begin{aligned}
&\int_{-\infty}^{\infty} dx \int_{-\infty}^{\infty} dp\, W_1(x,p)\, W_2(x,p) \\
&\quad = \frac{1}{\pi^2} \int_{-\infty}^{\infty} dx \int_{-\infty}^{\infty} dp \int_{-\infty}^{\infty} dx' \int_{-\infty}^{\infty} dx'' \\
&\qquad e^{-2ip(x'+x'')} \langle x + \frac{x'}{2} | \rho_1 | x - \frac{x'}{2} \rangle \langle x + \frac{x''}{2} | \rho_2 | x - \frac{x''}{2} \rangle \\
&\quad = \frac{1}{\pi} \int_{-\infty}^{\infty} dx \int_{-\infty}^{\infty} dx' \int_{-\infty}^{\infty} dx'' \\
&\qquad \delta(x' + x'') \langle x + \frac{x'}{2} | \rho_1 | x - \frac{x'}{2} \rangle \langle x + \frac{x''}{2} | \rho_2 | x - \frac{x''}{2} \rangle \\
&\quad = \frac{1}{\pi} \int_{-\infty}^{\infty} dx \int_{-\infty}^{\infty} dx' \langle x + \frac{x'}{2} | \rho_1 | x - \frac{x'}{2} \rangle \langle x + \frac{x'}{2} | \rho_2 | x - \frac{x'}{2} \rangle \\
&\quad = \frac{1}{\pi} \int_{-\infty}^{\infty} dx^* \int_{-\infty}^{\infty} dx^{*\prime} \langle x^* | \rho_1 | x^{*\prime} \rangle \langle x^{*\prime} | \rho_2 | x^* \rangle \\
&\quad = \frac{1}{\pi} \int_{-\infty}^{\infty} dx^* \langle x^* | \rho_1 \rho_2 | x^* \rangle \\
&\quad = \frac{1}{\pi} \operatorname{Tr}[\rho_1 \rho_2]
\end{aligned} \tag{44}
$$

If at least one of the two corresponding states is pure, we can relate this overlap to the fidelity of the two states.

B.1.2 Negativity in the Wigner distribution

As discussed earlier, if the Wigner distribution is non-negative everywhere, the corresponding state is essentially classical in the sense that the state has classical statistical interpretation in both momentum and position at the same time.

(**Hudson's Theorem).** *The Wigner distribution $W(x,p)$ of a pure state is everywhere positive if and only if the position wave function ψ is the exponential of a quadratic polynomial.*

Proof. This proof was first done in [Hud74].
We define a Gaussian position wave function with $e^{-\frac{c}{2}}$ as the normalization factor:

$$\psi_{a,b}(x) = e^{-\frac{1}{2}(ax^2+2bx+c)} \quad \text{with } \operatorname{Re}(a) > 0 \tag{45}$$

Similar to the calculations for the Wigner distribution of a coherent state in section B.1.3, we can show that the Wigner function of $\psi_{a,b}$ is a two-dimensional Gaussian function and hence, everywhere non-negative. In the following, we will prove that the Wigner distribution is only non-negative if ϕ is the exponential of a quadratic polynomial. Therefore, we will assume W_ϕ to be non-negative. Then we know, that the overlap of it with the Gaussian Wigner distribution

$W_{1,z}$ of the state $\psi_{1,z}$ is strictly positive and through equation (44) we know that:

$$\int_{-\infty}^{\infty} dx \int_{-\infty}^{\infty} dp\, W_\phi(x,p)\, W_{1,z}(x,p) = \frac{1}{\pi} |\, \langle \phi | \psi_{1,z} \rangle \,|^2 > 0 \tag{46}$$

We define $F : \mathbb{C} \to \mathbb{C}$:

$$F(z) = \int dx\ \bar{\phi}(x)\ e^{-\frac{1}{2}x^2 - zx} = e^{\frac{c}{2}}\ \langle \phi | \psi_{1,z} \rangle \tag{47}$$

First, we realize that F is entire, and we define a new entire function $g(z) = \frac{F'(z)}{F(z)}$, which is possible because $F(z)$ has no zeros. Then $G(z)$ as the anti-derivative of $g(z)$ is also entire and:

$$\frac{F(z)}{e^{G(z)}} = F(z) \cdot \frac{-1}{e^{2G(z)}} \cdot e^{G(z)} \cdot g(z) + F'(z) \cdot e^{-G(z)} = 0 \tag{48}$$

Now, we can choose $G(0)$ such that $F(0) = e^{G(0)}$ and we there exists an entire function $G(z)$ with:

$$F(z) = e^{G(z)} \tag{49}$$

Also, using Schwarz's inequality we get:

$$\begin{aligned} |F(z)|^2 &\leq ||\phi||^2 \cdot \int_{-\infty}^{\infty} dx\ e^{-x^2 - (\bar{z}+z)x} \\ &= ||\phi||^2 \cdot \int_{-\infty}^{\infty} dx\ e^{-(x+(\mathrm{Re}\ z))^2} e^{(\mathrm{Re}\ z)^2} = ||\phi||^2\ \sqrt{\pi} e^{(\mathrm{Re}\ z)^2} \end{aligned} \tag{50}$$

Finally, expressing $G(z)$ in equation (49) as a power series lets us conclude that $G(z)$ is a polynomial of up to second order.

$$\implies F(z) = e^{ax^2 + bx + k} \tag{51}$$

With $\tilde{z} = iz$ we interpret

$$F(\tilde{z}) = e^{-a\tilde{z}^2 + ib\tilde{z} + k} = \int dx\ \bar{\phi}(x)\ e^{-\frac{1}{2}x^2 - i\tilde{z}x} \tag{52}$$

as a Fourier transform of

$$F^*(x) = \bar{\phi}(x)\ e^{-\frac{1}{2}x^2} \tag{53}$$

Fourier transforms are Gaussian if and only if the considered function is also Gaussian and therefore $\bar{\phi}(x)\ e^{-\frac{1}{2}x^2}$ and $\bar{\phi}(x)$ are Gaussian, which is what we wanted to show. □

B.1.3 Wigner distribution of coherent and Cat states

Let us look at a coherent state $\rho = |\beta\rangle\langle\beta|$: Using equations (34) and (35) we can compute the Wigner function by:

$$\begin{aligned}
W^{|\beta\rangle\langle\beta|}(\alpha) &= \frac{1}{\pi^2}\int d^2\lambda\ \mathrm{Tr}(|\beta\rangle\langle\beta| e^{\lambda\hat{a}^\dagger - \lambda^\star\hat{a}})\ e^{\alpha\lambda^\star - \alpha^\star\lambda} \\
&= \frac{1}{\pi^2}\int d^2\lambda\ e^{-\lambda^2/2}\ \langle\beta| e^{\lambda\hat{a}^\dagger} e^{-\lambda^\star\hat{a}} |\beta\rangle\ e^{\alpha\lambda^\star - \alpha^\star\lambda} \\
&= \frac{1}{\pi^2}\int d^2\lambda\ e^{-\lambda^2/2}\ e^{\lambda(\beta^* - \alpha^\star)} e^{-\lambda^\star(\beta-\alpha)} \\
&\overset{\lambda=\lambda'+i\lambda'',\ x=\beta-\alpha}{=\!=\!=} \frac{1}{\pi^2}\int d^2\lambda\ e^{-(\lambda'^2+\lambda''^2)/2}\ e^{\lambda x^* - \lambda^* x} \\
&\overset{x=x'+ix''}{=\!=\!=} \frac{1}{\pi}\int d\lambda' e^{-\lambda'^2/2}\ e^{2i\lambda' x''} \cdot \frac{1}{\pi}\int d\lambda'' e^{-\lambda''^2/2}\ e^{2i\lambda'' x'} \\
&= \sqrt{\frac{2}{\pi}} e^{-2x''^2} \cdot \sqrt{\frac{2}{\pi}} e^{-2x'^2} \\
&= \frac{2}{\pi} e^{-2|\beta-\alpha|^2}
\end{aligned} \tag{54}$$

Superpositions of coherent states are called Cat states:

$$|\Psi^\phi_{\mathrm{cat}}\rangle = \frac{1}{\sqrt{N_\phi}}\left(|\beta\rangle + e^{i\phi}|-\beta\rangle\right) \tag{55}$$

with correct normalization:

$$N_\phi = 2(1+\cos(\phi)e^{-2|\beta|^2}) \tag{56}$$

$$\begin{aligned}
W^{\mathrm{cat},\phi}(\alpha) = \frac{1}{\pi^2 N_\phi}\int d^2\lambda\, e^{\alpha\lambda^* - \alpha^*\lambda}\Big(&\langle\beta| D(\lambda)|\beta\rangle + \langle-\beta| D(\lambda)|-\beta\rangle \\
&+ e^{i\phi}\langle\beta| D(\lambda)|-\beta\rangle + e^{-i\phi}\langle-\beta| D(\lambda)|\beta\rangle\Big)
\end{aligned} \tag{57}$$

Similar computation as in the example of coherent states leads to:

$$\begin{aligned}
W^{\mathrm{cat},\phi}(\alpha) = &\frac{1}{\pi\left(1+\cos(\phi)e^{-2|\beta|^2}\right)}\times \\
&\left[e^{-2|\alpha-\beta|^2} + e^{-2|\alpha+\beta|^2} + 2e^{-2|\alpha|^2}\cos\Big(4(\alpha''\beta' - \alpha'\beta'') + \phi\Big)\right]
\end{aligned} \tag{58}$$

As mentioned in the beginning of this section, in the Python library *qutip*, a different convention for the Wigner function is used. Compared to the convention used is the previous section, the graph of the Wigner function is stretched

by a factor of $\sqrt{2}$ in x and p direction and shrunk to $1/2$ of the function value. That way, the area under the graph remains constant. For the Wigner function with the *qutip* convention W_{qutip}, we can formally write:

$$W_{qutip}(\alpha) = \frac{1}{2} W\Big(\frac{\alpha}{\sqrt{2}}\Big) \tag{59}$$

Because *qutip* is used for the simulations in this work, their convention will be used.

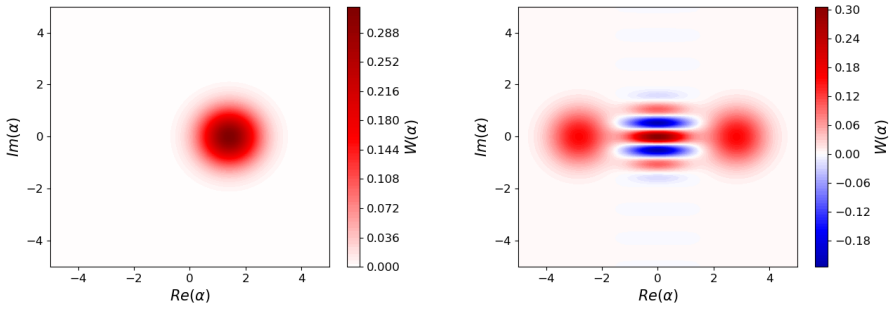

(a) Wigner function of the coherent state $|\alpha = 1\rangle$

(b) Wigner function of the even cat state $(\phi = 0)$ for $\alpha = 2$

Figure 12: Plots of Wigner functions for a coherent and a cat state; *qutip* convention is used for both plots

B.2 Lindblad master equation

We are describing an open system A coupled to an environment E in thermal equilibrium. The state of system A ρ_A can be recovered from tracing out the environment in the density matrix ρ_{AE} of the whole system $A + E$ that undergoes a unitary transformation. The goal is to find a first-order differential equation for ρ_A to conveniently describe the dynamics of A without monitoring the environment.

B.2.1 Markov approximation

Having a differential equation means that we can define our evolution in arbitrarily fine steps.

$$\tau \frac{d\rho_A(t)}{dt} = \rho_A(t+\tau) - \rho_A(t) \quad \text{for} \quad \tau \to 0 \tag{60}$$

Then the Hamiltonian for system and environment would lead to a density matrix of the following general form:

$$\rho_{AE}(t) = \rho_A(t) \otimes [\bar{\rho}_E + \delta\rho_E(t)] + \delta\rho_{AE}(t) \tag{61}$$

$\delta\rho_E(t)$ is some fluctuation around the steady-state value of ρ_E because of the interaction with A. Also, the Hamiltonian generally causes entanglement of A and E, which is described by the term $\delta\rho_{AE}(t)$

However, because of energy-time uncertainty, there is a correlation time of the environment of the order of $\tau_c = \frac{1}{\Delta\omega}$ with energy levels of the environment spanning over the range of $\Delta E = \hbar\Delta\omega$. If the steps in the differential equation are much longer than the environment correlation time, environment fluctuations average out and we can reduce the total density matrix to:

$$\rho_{AE}(t) = \rho_A(t) \otimes \rho_E \tag{62}$$

For this approximation of fixed minimal step length to be valid, the environment cannot significantly change the system's state during that correlation time. Therefore, we have the inequality:

$$\tau_c \ll \tau \ll T_r \tag{63}$$

where T_r is the characteristic time of the evolution of ρ_A. The Markov condition that $\tau_c \ll T_r$ is satisfied in cavity quantum electrodynamics and our case of realizing a Kerr-cat qubit.

B.2.2 Derivation and interpretation of the Lindblad equation

We can now write:

$$\frac{d\rho_A(t)}{dt} = \frac{\mathcal{L}_\tau[\rho_A(t)] - \rho_A(t)}{\tau} \tag{64}$$

where $\mathcal{L}_\tau[\rho_A(t)]$ is the operator for linear evolution of $\rho_A(t)$ in time τ. That is why we will now neglect all terms of order $O(\tau^2)$. We will use the Kraus representation for this channel, and because we want the channel to implement an infinitesimal change, we have exactly one operator of the order of unity.

$$\mathcal{L}_\tau[\rho_A(t)] = \sum_{\mu=0}^{N_K-1} M_\mu(\tau)\rho_A(t)M_\mu^\dagger(\tau) \tag{65}$$

with

$$M_0 = 1 - iK\tau \tag{66}$$

If we split K into hermitian and non-hermitian part ($K = \frac{H}{\hbar} - iJ$), we get:

$$M_0(\tau)\rho_A M_0^\dagger(\tau) = \rho_A - \frac{i\tau}{\hbar}[H, \rho_A] - \tau(J\rho_A + \rho_A J) \tag{67}$$

The other Kraus operators are of order τ ($M_\mu(\tau) = \sqrt{\tau}L_\mu$). Normalization of the Kraus operators leads to:

$$\sum_{\mu=0}^{N_K-1} M_\mu^\dagger(\tau)M_\mu(\tau) = \mathbf{I} - 2J\tau + \sum_{\mu\neq 0} \tau L_\mu^\dagger L_\mu = \mathbf{I} \tag{68}$$

$$\implies J = \frac{1}{2}\sum_{\mu\neq 0} L_\mu^\dagger L_\mu \tag{69}$$

Finally, we get the Lindblad master equation:

$$\frac{d\rho_A}{dt} = -\frac{i}{\hbar}[H_A, \rho] + \sum_{\mu\neq 0}\left(L_\mu \rho_A L_\mu^\dagger - \frac{1}{2}L_\mu^\dagger L_\mu \rho_A - \frac{1}{2}\rho_A L_\mu^\dagger L_\mu\right) \tag{70}$$

The hermitian H_A can be identified as the system's Hamiltonian. To interpret the Kraus operators, we realize that we can model the evolution of system A equivalently as the unitary evolution of system and environment $A+E$ and as the unitary evolution U_{AB} of system and environment simulator $A+B$.

$$\begin{aligned} U_{AB}\,|\phi^{(A)}\rangle \otimes |0^{(B)}\rangle &= M_0(|\phi^{(A)}\rangle) \otimes |0^{(B)}\rangle + \sum_{\mu\neq 0} M_\mu(|\phi^{(A)}\rangle) \otimes |\mu^{(B)}\rangle \\ &= \Big[\mathbf{I} - \frac{i}{\hbar}H_A\tau - J\tau\Big](|\phi^{(A)}\rangle) \otimes |0^{(B)}\rangle + \sqrt{\tau}\sum_{\mu\neq 0} L_\mu(|\phi^{(A)}\rangle) \otimes |\mu^{(B)}\rangle \end{aligned} \tag{71}$$

If we were now to read out the environment we would find it with a probability p_μ in the state $|\mu^{(B)}\rangle$. It is important to note that with a high probability, the environment simulator stays in the same state as before the transformation. In this case, the system's state evolves under an effective Hamiltonian $H_A - i\hbar J$. The other Kraus operators with $\mu \neq 0$ change the environment's state and, therefore, correspond to leakage into the environment.

B.3 Input-Output Formalism

In the Schrödinger picture, we study the evolution of open quantum systems with the Lindblad master equation. In the Heisenberg picture, we can analyze input and output fields using input-output formalism. We consider a cavity with resonance frequency ω_c that is coupled to an external environment, such that the Hamiltonian decomposes into:

$$H = H_{cav} + H_{ext} + H_{int} \tag{72}$$

with

$$H_{cav}/\hbar = \omega_c a^\dagger a \tag{73}$$

$$H_{ext}/\hbar = \int_0^\infty d\omega'\ \omega' b^\dagger(\omega') b(\omega') \tag{74}$$

$$H_{int}/\hbar = \frac{1}{2\pi}\int_0^\infty d\omega' \sqrt{\kappa(\omega')}\Big(a b^\dagger(\omega') + a^\dagger b(\omega')\Big) \tag{75}$$

By making the rotating wave approximation, we can omit the terms $a^\dagger b^\dagger(\omega')$ and $ab(\omega')$. We expect only bath modes with $\omega' \approx \omega_c$ to contribute ($b(\omega') \approx 0$ for $\omega' \not\approx \omega_c$) and hence, we can extend the lower bounds in both integrals to

$-\infty$.

With this Hamiltonian, the Heisenberg equations of motion state:

$$\begin{aligned}\partial_t a &= -\frac{i}{\hbar}[a, H_{cav}] - \frac{i}{\hbar}[a, H_{int}] \\ &= -i\omega_c a(t) - \frac{i}{\sqrt{2\pi}} \int_{-\infty}^{\infty} d\omega' \ \sqrt{\kappa(\omega')} b(\omega') \end{aligned} \tag{76}$$

$$\begin{aligned}\partial_t b(\omega') &= -\frac{i}{\hbar}[b, H_{ext}] - \frac{i}{\hbar}[b, H_{int}] \\ &= -i\omega' b(\omega') - i\sqrt{\frac{\kappa(\omega')}{2\pi}} a(t) \end{aligned} \tag{77}$$

Transforming equation (77) to the rotating frame at frequency ω' and integration leads to:

$$b(\omega', t) = b(\omega', t_0) e^{-i\omega'(t-t_0)} - i\sqrt{\frac{\kappa(\omega')}{2\pi}} \int_{t_0}^{t} dt' \ a(t') e^{-i\omega'(t-t')} \tag{78}$$

Inserting this expression for the bath modes into equation (76), we get to the final exact expression:

$$\begin{aligned}\partial_t a = -i\omega_c a(t) \ - \ & \frac{i}{\sqrt{2\pi}} \int_{-\infty}^{\infty} d\omega' \ \sqrt{\kappa(\omega')} b(\omega', t_0) e^{-i\omega'(t-t_0)} \\ & - \frac{1}{2\pi} \int_{-\infty}^{\infty} d\omega' \ \kappa(\omega') \int_{t_0}^{t} dt' \ a(t') e^{-i\omega'(t-t')} \end{aligned} \tag{79}$$

To make progress and simplify the terms, we can assume $\kappa(\omega')$ to be constant over all frequencies. This approximation can be made because there is usually only a small range of frequencies that contribute similarly, for example, the frequencies of the resonance linewidth for the interaction with an optical cavity. Then, the equation results in what is known as the quantum Langevin equation:

$$\partial_t a = -i\omega_c a(t) - \frac{\kappa}{2} a(t) - \sqrt{\kappa} a_{\text{in}}(t) \tag{80}$$

with

$$a_{\text{in}}(t) := \frac{i}{\sqrt{2\pi}} \int_{-\infty}^{\infty} d\omega' \, b(\omega', t_0) e^{-i\omega'(t-t_0)} \tag{81}$$

$a_{\text{in}}(t)$ describes how past bath modes couple to the system at time t and interpret it as a noise contribution with $\langle a_{\text{in}}(t) \rangle = 0$ and $[a_{\text{in}}(t), a_{\text{in}}^{\dagger}(t')] = \delta(t-t')$ We can also find a time-reversed quantum Langevin equation, which describes the evolution of the system via the outcoming field:

$$\partial_t a = -i\omega_c a(t) + \frac{\kappa}{2} a(t) - \sqrt{\kappa} a_{\text{out}}(t) \tag{82}$$

with

$$a_{\text{out}}(t) := \frac{i}{\sqrt{2\pi}} \int_{-\infty}^{\infty} d\omega' \, b(\omega', t_1) e^{-i\omega'(t-t_1)} \quad \text{with} \quad t_1 > t \tag{83}$$

This can be interpreted as the future bath modes coupling to the system at time t.

Furthermore, there is the fundamental input-output relation between input and output fields:

$$a_{\text{out}}(t) - a_{\text{in}}(t) = \sqrt{\kappa}\, a(t) \tag{84}$$

B.4 Quantum Stochastic Calculus

Quantum Stochastic Calculus (QSC) is a mathematically rigorous description of open quantum systems that treats a system's interaction with an environment as a continuous stochastic process with quantum jumps. The detailed discussion of this topic can be found in [ZG97]. With this theory, we can recover both the Lindblad master equation as well as the quantum Langevin equation.

We assume the same Hamiltonian as in section B.3. By making the rotating-wave approximation and the Markov approximation, we can write the interaction part of the Hamiltonian (absorbing constant in c) as:

$$H_{\text{int}}(t) = i\Big(b(t)^\dagger a - b(t) a^\dagger\Big) \quad \text{with} \quad b(t) = \frac{1}{\sqrt{2\pi}} \int_{-\infty}^{\infty} d\omega \; b(\omega) e^{-i(\omega-\omega_c)t} \tag{85}$$

The time evolution operator is given by the Schrödinger equation:

$$\frac{d}{dt} U(t) = -i(H + H_{\text{int}}(t)) U(t) \tag{86}$$

We define analogous to the classical Wiener process stochastic increments $dB(t)$ and $dB(t)^\dagger$ that represent a random change following a normal distribution:

$$B(t) := \int_0^t ds \, b(s), \quad B(t)^\dagger := \int_0^t ds \, b(s)^\dagger \tag{87}$$

and with that:

$$dB(t) = B(t+dt) - B(t), \quad dB(t)^\dagger = B(t+dt)^\dagger - B(t)^\dagger \tag{88}$$

We usually consider the environment in the vacuum $|0\rangle$ state, such that $\langle b(t) \rangle = \langle 0 | \, b(t) \, | 0 \rangle = 0$, $\langle b(t)^\dagger \rangle = 0$, $\langle b^\dagger(t) b(t') \rangle = 0$ and $\langle b(t) b(t')^\dagger \rangle = \delta(t - t_0)$.

Importantly, that gives us:

$$\langle dB(t) dB(t)^\dagger \rangle = dt \tag{89}$$

which means that differentials must be expanded to second order.

Here, we will not get into the details of Ito and Stratonovich integration, but the idea now is to substitute $dB(t)$ for $b(t)$ in equation (85) and to solve

equation (86), which has now become a Stochastic Differential Equation.

Finally, we derive the equation of motion stochastic density operator, which generates the master equation:

$$\begin{aligned} d\hat{\rho}(t) = -i\left(H_{\text{eff}}\hat{\rho}(t) - \hat{\rho}(t)H_{\text{eff}}^{\dagger}\right)dt + dB(t)^{\dagger}a\hat{\rho}(t)a^{\dagger}dB(t) \\ + dB(t)^{\dagger}a\hat{\rho}(t) + \hat{\rho}(t)dB(t)a^{\dagger} \end{aligned} \tag{90}$$

with

$$H_{\text{eff}} = H_{\text{system}} - \frac{i}{2}a^{\dagger}a \tag{91}$$

From tracing out the bath environment, we recover the Lindblad master equation.

We can similarly derive the Ito quantum Langevin equation from knowledge of the time evolution operator. For an arbitrary operator $X(t)$ in the Heisenberg picture:

$$dX(t) = -i\left[X, H_{\text{sys}}\,dt + idB(t)a^{\dagger} - idB(t)^{\dagger}a\right] + \left(a^{\dagger}Xa - \frac{1}{2}Xa^{\dagger}a - \frac{1}{2}a^{\dagger}aX\right)dt \tag{92}$$

We can derive the quantum Langevin equation in the standard form by setting $X = a$.

B.4.1 Output processes

Output processes can be formalized in QSC with

$$B_{\text{out}}(t) := \hat{U}(t)^{\dagger}B(t)\hat{U}(t) \tag{93}$$

such that the output field can be written as:

$$b_{\text{out}}(t) := \frac{dB_{\text{out}}(t)}{dt} \equiv \lim_{h\to 0^{+}} \frac{B_{\text{out}}(t+h) - B_{\text{out}}(t)}{h} \tag{94}$$

We can finally derive an equation that fully describes the output process:

$$dB_{\text{out}}(t) = B_{\text{out}}(t+dt) - B_{\text{out}}(t) = dB(t) + c(t)\,dt \tag{95}$$

C Code

All my codes with documentation can be found on GitHub. The most important ones are listed additionally in this section.

C.1 Code: Negativity in terms of K*Q *qutip* simulation

This code generates the red line in figure 4. To use the function in different plots (figure 4 and 6) we use the function *joblib.dump*. With a slight code modification, we can also generate the red line in 5.

```
from qutip import *
import numpy as np
import matplotlib.pyplot as plt
from numpy import pi, sqrt
from scipy import interpolate
from joblib import dump

N = 30  # fock state truncation
omega = 2 * pi * 5e9  # resonance frequency


# function that returns the end max negativity for given
    parameters of the initialization process
# inputs K,kappa,e2 in unit 1/s
# time_param dimensionless parameter that characterizes and
    is linearly proportional to the duration of the turn-up (
    read in detail in Bachelor's thesis)
# different convention for K - watch out
def wigner_negativity(K, kappa, e2, time_param):
    a = destroy(N)  # destruction operator
    H0_init = -K * a.dag() * a.dag() * a * a  # non time-
        varying part of the Hamiltonian

    # time-varying part of the Hmailtonian with coefficient
        the captures the time-variation
    H1_init = e2 * (a.dag() ** 2 + a**2)

    def H1_init_coeff(t, args):
        return 1 / 2 * np.tanh((t - 4 * time_param / K) * (K
            / time_param)) + 1 / 2

    # complete Hamiltonian
    H_init = [H0_init, [H1_init, H1_init_coeff]]

    # time scale for numerical solving of the master
        equation
    # details in Bachelor's thesis
    times = np.linspace(0, (6 * time_param) / K, 200)

```

```
    opt = {
        "nsteps": 3000
    }  # steps of the integration (needs to be increased for certain computations)

    # mesolve (see documentation qutip: Master equation), c_ops are complete list of loss operators
    time_ev = mesolve(
        H_init, fock(N, 0), tlist=times, c_ops=sqrt(kappa) * a, args=None, options=opt
    )

    end_state = time_ev.states[-1]  # end state of initialization via Master equation

    # evaluate Wigner negativity on the axis (Re a=0 or y-axis) for x=0
    x_gridspace = np.linspace(0, 0, 1)
    y_gridspace = np.linspace(-2, 2, 500)
    W_end_state = wigner(end_state, x_gridspace, y_gridspace)
    wigner_values = [
        W_end_state[i, 0] for i in range(500)
    ]  # negativity maximal on Re(a)=0

    return -min(wigner_values)


# returns for given K and Q the minimum value of wigner funciton that is possible to reach with optimizing over e2 (second output is the e2 value in Hz that optimizes Wigner negativity)
def max_wigner_negativity_optimized_over_e2(K, kappa, time_param):
    # empirically we could test that photon numbers lower than 0.8 and higher than 8 don't lead to higher negativity (increasing range of e2 values doesn't affect results)
    e2_values = np.linspace(0.8 * K, 8 * K, 60)  # array with e2s with optimize over
    negativity_values = np.array(
        [wigner_negativity(K, kappa, e2, time_param) for e2 in e2_values]
    )  # array with all Wigner negativity value for the possible e2s

    # find max and the e2 value that maximizes negativity
    max_negativity_value = np.max(negativity_values)
    max_e2 = e2_values[np.argmax(negativity_values)]
    return max_negativity_value, max_e2 / (2 * pi)
```

```
67
68
69  # plot K*Q in Hz versus optimized negativity
70  # read in thesis why initialization negativity only depends
        on product K*Q
71  # K is set to 500 kHz
72  KQ_array_Hz = np.logspace(np.log10(7 * 10**9), np.log10(2 *
        10**12), 100)
73  K_fixed = 5e5
74  kappa_array = omega / (KQ_array_Hz / (K_fixed))
75  optimized_negativity = [
76      max_wigner_negativity_optimized_over_e2(2 * pi * K_fixed
            , kappa_array[i], 2)[0]
77      for i in range(len(kappa_array))
78  ]
79  plt.plot(KQ_array_Hz, optimized_negativity)
80
81
82  # we want to have the this function (Negativity vs K*Q) for
        other plots so we dump it with joblib.dump and plot it to
         ensure a correct fit
83  f = interpolate.interp1d(KQ_array_Hz, optimized_negativity)
84  dump(f, "Negativity(KQ) 100 values newest")
85  plt.plot(KQ_array_Hz, f(KQ_array_Hz), color="red")
86
87  # plot appearance
88  plt.xscale("log")
89  plt.xlabel("K*Q in Hz")
90  plt.ylabel("Max negativity in Wigner function")
91
92  plt.grid(True, which="both", linestyle=":", linewidth=0.5,
        color="gray")
93  plt.tick_params(axis="both", which="both", direction="in",
        length=6, width=1)
94  plt.minorticks_on()
95  plt.show()
```

Listing 1: Negativity in terms of K*Q for *qutip* simulation

C.2 Code: Negativity in terms of K*Q calculation for adiabatic evolution and *qutip* simulation for comparison (figure 4)

This code generates figure 4, and with some minor modifications, figure 5.

```
1  import numpy as np
2  from scipy.integrate import odeint
3  import matplotlib.pyplot as plt
4  from numpy import pi
```

```
from numpy import tanh
from scipy import interpolate
from joblib import dump
from joblib import load

omega = 2 * np.pi * 5 * 1e9  # resonance frequency


# derivation of the differential equation for the negativity during turn up is explained in detail in Bachelor's thesis
def DEQ_Negativity(n, t, K, e2, kappa, time_param):
    # alpha2_t means alpha(t)**2
    alpha2_t = e2 / (2 * K) * (tanh((t - 4 * time_param / K) * K / time_param) + 1)
    # differential equation for increasing negativity due to increasing alpha
    increase = (
        n
        * pi**2
        * e2
        / (16 * alpha2_t**2 * time_param)
        * (1 - tanh((t - 4 * time_param / K) * K / time_param) ** 2)
    )
    # differential equation for decreasing negativity due to photon loss
    decrease = -2 * alpha2_t * kappa * n
    # complete differential equation
    dNegdt = increase + decrease
    return dNegdt


# solve DEQ for the system parameters (no optimizing over e2 yet)
# starting value of the numerical integration is explained in detail in Bachelor's thesis, but short explanation inside function
# return end negativity
def max_wigner_DEQ(K, e2, kappa, time_param):
    # numerical integration starts at time 3 * time_param / K, if it starts earlier, negativity values are very small and numerical integration fails (gives wrong result)
    t = np.linspace(3 * time_param / K, 6 * time_param / K, 1000)
    # calculation of Wigner negativity at the start of the integration, can be calculated because the start state is almost the cat state as there for small alpha photon loss is negligible
```

```
    n0 = 1 / pi * np.exp(-(pi**2) * K / (4 * 0.24 * e2))
    # numerical integration
    n = odeint(DEQ_Negativity, n0, t, args=(K, e2, kappa,
        time_param))
    return n[-1]


# optimize negativity over e2 (corresponding to photon
    number of the end state)
def max_wigner_optimized_over_e2_DEQ(K0, kappa0, time_param)
    :
    # create a list of all negativity values for the e2's
    list_max_wigner_optimized_over_e2 = [
        max_wigner_DEQ(K0, i, kappa0, time_param)
        for i in np.linspace(K0 * 0.8, 7 * K0, 50)
    ]
    # return the max negativity value and the e2 in Hz for
        which we get this negativity
    return max(list_max_wigner_optimized_over_e2), np.
        linspace(0.8 * K0, 7 * K0, 50)[
        list_max_wigner_optimized_over_e2.index(max(
            list_max_wigner_optimized_over_e2))
    ] / (2 * pi)


# define the axis K*Q
KQ_array = np.logspace(np.log10(7 * 10**9), np.log10(2 *
    10**12), 100)
# like for the qutip simulation, fix a K and go over kappa
    instead of K*Q (because optimized negativity is only
    dependent on K*Q)
K_fixed = 5e5
kappa_array = omega / (KQ_array / (K_fixed))

# generate the optimized negativity values for given K and
    kappa and therefore given K*Q
optimized_negativity_values_DEQ = [
    max_wigner_optimized_over_e2_DEQ(2 * pi * K_fixed,
        kappa_array[i], 2)[0]
    for i in range(len(kappa_array))
]

# plot the optimized negativity values against K*Q
plt.plot(
    KQ_array,
    optimized_negativity_values_DEQ,
    color="black",
    label="Calculation for adiabatic evolution",
)

```

```
78
79 # plot for comparison the Negativity values we got from the
       qutip simulation
80 # load the function that gives Negativity in terms of K*Q
       for the qutip simulation
81 Negativity_KQ_qutip = load("Negativity(KQ) 100 values newest
       ")
82 plt.plot(KQ_array, Negativity_KQ_qutip(KQ_array), color="red
       ", label="qutip simulation")
83
84 # plot appearance
85 plt.xscale("log")
86 plt.xlabel("K*Q in Hz")
87 plt.ylabel("Maximum Wigner negativity")
88
89 plt.legend()
90
91 plt.grid(True, which="both", linestyle=":", linewidth=0.5,
       color="gray")
92 plt.tick_params(axis="both", which="both", direction="in",
       length=6, width=1)
93 plt.minorticks_on()
94
95 plt.show()
```

Listing 2: Negativity in terms of K*Q for calculation (assumption of adiabatic evolution) and for the *qutip* simulation for comparison

C.3 Code: Modification of the previous code for the alternative model described in section 3.2

For the alternative and easier way of calculating Wigner negativity for adiabatic evolution, the function *max_wigner_DEQ* from the previous code must be changed as follows.

```
1 import numpy as np
2 from numpy import tanh, exp, pi
3 from scipy.integrate import odeint
4
5
6 # alternative (easier) way to calculate Wigner negativity
      for adiabatic evolution
7 # we only show the part of the code that changes
8 def max_wigner_DEQ(K, e2, kappa, time_param):
9     times = np.linspace(0, 6 * time_param / K, 1000)  # time
          steps of the evolution
10
11    # describing photon loss through a differential equation
          as explained in the Bachelor's thesis
```

```
    def photon_loss_differential_description(n, t):
        alpha2_t = e2 / (2 * K) * (tanh((t - 4 * time_param
            / K) * K / time_param) + 1)
        decrease = -2 * alpha2_t * kappa * n
        return decrease

    # solving the differential equation
    photon_loss_factor = odeint(
        photon_loss_differential_description, 1, times)

    # Wigner negativity decrease due to photon loss must be
        multiplied by Wigner negativity of alpha cat state
    # to good approximation it is given by the following
        expression
    def negativity_alpha_cat_state(t):
        alpha2_t = e2 / (2 * K) * (tanh((t - 4 * time_param
            / K) * K / time_param) + 1)
        return 1 / pi * exp(-(pi**2) / (8 * alpha2_t))

    # return the last value (end of initialization) for the
        Wigner negativity
    negativity_t = (
        np.array(negativity_alpha_cat_state(times))
        * np.array(photon_loss_factor).flatten()
    )
    return negativity_t[-1]
```

Listing 3: Code change compared to Listing C.2 for the alternative way of calculating Wigner negativity

C.4 Code: Dephasing constant for initialized state with parameters K and Q

This code generates figure 11. With modications of the noise rates or replacing dephasing decay constants with dephasing times, we can also generate figures 9, 10 and 8.

```
from qutip import *
import numpy as np
import matplotlib.pyplot as plt
import math
from math import pi
from math import sqrt
from joblib import load
from scipy.optimize import curve_fit
from matplotlib.lines import Line2D

# load the function that gives the photon number for optimal
    initialization
```

```
n_KQ = load("n(KQ) qutip 100 values interpolation newest")


# to get alpha we take the sqrt, for values of K*Q smaller than 7e9 Hz we dont care about the dephasing time because the initialized state doesn't have Negativity in the Wigner function
# we set the value alpha value for K*Q = 7e9
def alpha(KQ):
    if KQ > 7 * 1e9:
        return sqrt(n_KQ(KQ))
    else:
        return sqrt(0.92)


N = 20  # Fock state truncation
omega = 2 * pi * 5 * 1e9  # resonance frequency


# goal: simulate decay time of the coherent alpha state to get dephasing time for KCQ
# therefore plot the x expectation value against time and fit an exponential decay
# function takes characteristic system parameters K in Hz and Q
# function assumes thermal nuumber and kappa_eff (rate for a ^dagger * a noise) to be the same as in Grimm paper
def dephasing_time(K_Hz, Q):
    # calculate related system parameters from K and Q (alpha value such that we have maximum negativity)
    K = K_Hz * 2 * pi
    alpha_value = alpha(K_Hz * Q)
    e2 = K * alpha_value**2  # calculate the e2 of the optimal initialization
    kappa = omega / Q  # photon loss rate
    kappa_thermal = kappa * 0.08  # photon gain rate
    kappa_eff = 2 * pi * 230  # rate of a^dagger a noise

    a = destroy(N)  # destruction operator
    x = (a + a.dag()) / 2  # x operator

    H_cat = -K * a.dag() * a.dag() * a * a + e2 * (
        a.dag() ** 2 + a**2
    )  # static Hamiltonian

    times = np.linspace(0, 1e-6 * 150, 400)  # time scale of system evolution

    opt = {
        "nsteps": 7000
```

```
    }  # number of steps in numerical solving of the master equation

    # master equation solver, coherent alpha state is the initial state, loss operators corresponding to the noise processes, e_ops=[x] gives the x expectation value for each time in times
    time_ev = mesolve(
        H_cat,
        coherent(N, alpha_value),
        tlist=times,
        c_ops=[
            sqrt(kappa) * a,
            sqrt(kappa_thermal) * a.dag(),
            sqrt(kappa_eff) * a.dag() * a,
        ],
        e_ops=[x],
        args=None,
        options=opt,
    )

    # fit exponential decay (at t=0 the x expectation value of the coherent state is alpha), c is the dephasing constant
    def fitted_exponential(x, c):
        return alpha_value * np.exp(-x * c)

    dephasing_time_value, _ = curve_fit(fitted_exponential, times, time_ev.expect[0])
    print(dephasing_time_value[0])
    return dephasing_time_value[0]


# make a K,Q grid
K = np.linspace(0.5e5, 10e5, 10)
Q = np.linspace(0.5e5, 10e5, 10)


# Calculate the dephasing times for each pair (K, Q)
decay_constants = np.zeros((len(K), len(Q)))
for i in range(len(K)):
    for j in range(len(Q)):
        decay_constants[i, j] = dephasing_time(K[i], Q[j])

# Plot the contour plot with the given levels for the dephasing time
plt.figure(figsize=(8, 6))
viridis_r = plt.cm.get_cmap("viridis").reversed()
contour = plt.contour(
    K / 1e6,
```

```
    Q / 1e6,
    decay_constants.T,
    levels=np.array([6e3, 7e3, 8e3, 1e4, 1.5e4, 2.5e4, 5e4]),
    cmap=viridis_r,
    vmin=2e3,
    vmax=6.5e4,
)

# plot appearance
# plt.colorbar(contour, label=" KCQ Dephasing Time in " r"$\mu s$")
plt.xlabel("K in MHz")
plt.ylabel("Q in " r"$10^6$")

plt.grid(True, which="both", linestyle=":", linewidth=0.5, color="black")
plt.tick_params(axis="both", which="both", direction="in", length=6, width=1)
plt.minorticks_on()

# Legend description
legend_description = Line2D(
    [0], [0], linestyle="", label=r"$\text{Decay constant in } 1/s $"
)

# Contour legend labels
legend_labels = ["6000", "7000", "8000", "10000", "15000", "25000", "50000"]
legend_colors = [
    contour.collections[i].get_edgecolor() for i in range(len(legend_labels))
]
legend_handles = [
    Line2D([0], [0], linestyle="-", color=legend_colors[i])
    for i in range(len(legend_labels))
]

# Add description to the legend handles and labels
legend_handles.insert(0, legend_description)
legend_labels.insert(0, r"$\text{Decay constant in } 1/s $")

plt.legend(legend_handles, legend_labels)

plt.show()
```

Listing 4: Dephasing constant for initialized state with system parameter K, Q and noise rates as in [Gri+20]